

Understanding the nature of ULX with SIMBOL-X

Luigi Foschini

*Istituto di Astrofisica Spaziale e Fisica Cosmica (IASF) del CNR
Sezione di Bologna, Italy*

IASF–BO Internal Report n. 390

May 19, 2004

Revision History

v 1.0	First version.
19/05/2004	Talk held in Paris for the 1 st SIMBOL–X Workshop (11 – 12 March 2004)

1 Introduction

This report summarizes the scientific performances expected from SIMBOL-X in the observation of the ultraluminous X-ray sources (ULX). The basic concepts of the SIMBOL-X satellite are described in Ferrando et al. (2003) and references therein.

This report provides a preliminary evaluation of the scientific performances expected from the SIMBOL-X satellite according to the tests performed so far by extrapolating the spectra obtained with *XMM-Newton* at the energies of SIMBOL-X, by using the latest version of response matrices (18 February 2004).

2 The ultraluminous X-ray sources: current problems and open questions

The ultraluminous X-ray sources (ULX) are point sources with luminosity in the energy band 0.5–10 keV within the range 10^{39-41} erg/s and located sufficiently far from the dynamic centre of the host galaxy to avoid confusion with low luminosity AGN. Moreover, the ULX should be located inside the D_{25} ellipse of the host galaxy. Although there are some variants, this is the generally agreed definition, used by most of the researchers (cf Makishima et al. 2000, Miller & Colbert 2004).

The ULX were discovered already with *Einstein* satellite in '80 (Fabbiano et al. 1989). *ROSAT* and *ASCA* satellites gave a considerable contributions, but *Chandra* and *XMM-Newton* satellites offered the opportunity of a “revolution” in this research field (see Miller & Colbert 2004 for a history of ULX studies).

The reason of such a wide interest in ULX research is that these sources can potentially host intermediate mass black holes (IMBH), with masses between $10^2 - 10^4 M_\odot$. Miller et al. (2003a, 2003b) suggested that NGC1313 X-1 and X-2, and M81 X-9 could host intermediate mass black holes, with masses of the order of $10^2 - 10^3 M_\odot$, on the basis of the presence of a very soft thermal component ($kT \approx 0.1 - 0.2$ keV). In that case, according to the standard theory of the accretion disk, since the mass of the central object depends on the peak temperature (see below), the “cool” disk could be an indication of the presence of an IMBH. Indeed, as the disk is optically thick, to each radius corresponds an effective temperature:

$$T(r) = \left[\frac{3GM\dot{M}}{8\pi\sigma r^3} \left(1 - \sqrt{\frac{r_{in}}{r}}\right) \right]^{0.25} \quad (1)$$

where $T(r)$ is the temperature at the radius r , σ is the Stefan–Boltzmann constant, G is the Newton’s gravitational constant, M is the mass of the central object, \dot{M} is the accretion rate, and r_{in} is the radius of the innermost stable orbit, that for a Schwarzschild metric is 6 times the gravitational radius $r_g = GM/c^2$. In the case of Kerr metric, the radius can be down to $1.24r_g$.

Because of the comptonization in the disk atmosphere, the local temperature is a bit higher than the effective temperature. The ratio of the color temperature and the effective temperature is called *spectral hardening factor* (κ) and is generally equal to 1.7, increasing slightly with the accretion rate (Shimura & Takahara 1995). Moreover, it is necessary to take into account that the peak temperature at the innermost stable orbit occurs at a radius somewhat larger than r_{in} (therefore, the corrective factor ξ has to be introduced; see Kubota et al. 1998). By taking into account these two factors, it is possible to rearrange the Eq. (1) as:

$$T_{in} = 1.2 \sqrt{\frac{\xi}{0.41}} \frac{\kappa}{1.7} \frac{1}{\sqrt{\alpha}} \eta^{0.25} \left(\frac{M}{10M_\odot} \right)^{-0.25} \quad (2)$$

More details can be found in Makishima et al. (2000) or Ebisawa et al. (2003). The typical spectrum of the ULX is modelled with the multicolor accretion disk (`diskbb` in `xspec`) plus a power law, that generally mimic the comptonization process. Wang et al. (2004) have recently shown, with MonteCarlo simulations, that a single model of comptonized multicolor accretion disk is equivalent to the double component model multicolor disk plus a hard tail. However, several authors (e.g. Ebisawa et al. 2003) challenged this theory, suggesting that the above model can be efficiently substituted by a model of a “slim disk”, with superEddington accretion rate. The main result of this model is to constrain the mass of the central object to a few solar masses.

The stellar mass black hole is another common hypothesis in the ULX studies: indeed, in addition to the ULX with the “cool” disk, there is another class of object with a “too hot” disk, that is with temperature greater than 1 keV. It is known that for Galactic black holes in X-ray binaries (XRB) the temperature of the accretion disk is generally between 0.4 – 1 keV, while there are some ULX with temperature 1 – 1.5 keV, which in turn is consistent with Galactic microquasars. Therefore, in this case, the accretion rate is subEddington, but the high luminosity is likely to be due to different effects, like some kind of anisotropic emission, like relativistic jets (Georganopoulos et al. 2002) or simply anisotropies in the optical depth (King et al. 2001).

Another hypothesis to explain the high luminosity with stellar mass black holes and superEddington accretion rates is the presence of inhomogeneities driven by a strong radiation pressure, so that the escaping flux could exceed the Eddington limit by a factor of 10 – 100 (Begelman 2002).

Last, but not least, Makishima et al. (2000) suggested that the ULX could be explained by a spinning black hole, with high inclined disk ($i > 80^\circ$): in this case, the relativistic effects play a fundamental role in enhancing the luminosity.

To summarize, there are two main classes of ULX, both characterized by a thermal component plus a hard tail. The first class has the thermal component with low temperature ($T_{in} < 0.2 - 0.3$ keV, the “cool disk”): this is the most interesting class of ULX, since they could be IMBH or superEddington sources with a non-standard accretion disk. The second one has the thermal component with high temperature ($T_{in} \approx 1 \div 1.5$ keV, the “too hot disk”): these ULX are likely to be stellar mass black holes with some type of anisotropic emission. We could also add a third class, characterized by a simple power law spectrum (e.g. Foschini et al. 2002a). This third class is likely to be composed of active galactic nuclei or background (e.g. Foschini et al. 2002b, Masetti et al. 2003).

3 Why SIMBOL-X

3.1 What is available now to the observers

The ULX are generally difficult to observe with optical telescopes, since are located inside the galaxy bulges or behind dust lanes (e.g. NGC4565, Fig. 1). Radio counterparts have been found only in very few cases (e.g. Kaaret et al. 2003). Therefore, it is necessary to extract as many informations as possible from X-ray and possibly γ -ray observations.

Presently, *Chandra* and *XMM-Newton* are already doing a very good work below 10 keV, by giving to the observers the possibility to have good images at arcsecond resolution (*Chandra*, see the ULX in the Antennae galaxies, Fabbiano et al. 2001) and high signal-to-noise ratio spectra with energy resolution up to 70 – 80 eV (*XMM-Newton*, see for example M33 X-8, Foschini et al. 2004).

However, at energies greater than 10 keV the present satellites are not enough for this research field, both in sensitivity and angular resolution. RXTE has a collimated field of view with 1° size, while IBIS/ISGRI onboard INTEGRAL has a angular resolution of $12'$, sampled in $5'$ pixels. The latter is very good for

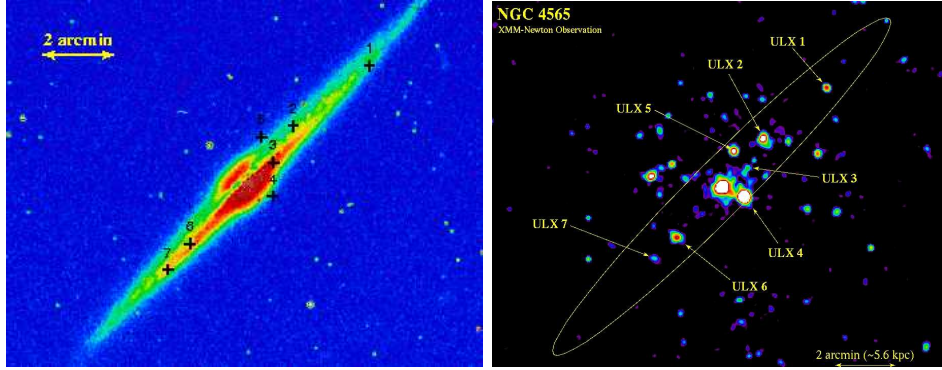


Figure 1: (left): NGC4565 from the Digitized Sky Survey. The crosses indicate the position of the ULX shown in the corresponding image from *XMM-Newton* (right). See Foschini et al. (2002a) for details on ULX in NGC4565.

coded-mask instruments, but not sufficient to avoid source confusion for sources outside the Milky Way, except for some particular cases. *SIMBOL-X* could fill this gap.

3.2 SIMBOL-X applied to ULX studies

SIMBOL-X could be of great advantage in studies of ULX, specifically at energies greater than 10 keV. The expected sensitivity of $\approx 1 \mu\text{Crab}$ at about 30 keV (3σ detection with 1 Ms exposure, $\Delta E = E/2$, Ferrando et al. 2003), together with a half-energy width (HEW) of $30''$, can give the necessary sensitivity and angular resolution to study the high energy emission from objects distant several megaparsecs. It would be better to reach HEW= $10''$ with the alternative design, so to avoid source confusion at high distance (see G. Hasinger 2004).

Moreover, the large energy band (0.5 – 70 keV) would allow to put tight constraints in the spectral parameters. A useful example is shown in Fig. 2 in the work by Georganopoulos et al. (2002): they performed a numerical simulation to calculate the spectrum of a ULX system like Cygnus X-1, with different parameters to explain the high energy emission (there modelled as coming from a jet). Observations in the energy band of SIMBOL-X (0.5 – 70 keV) could allow to distinguish between different parameters and also models (if the emission at energies greater than 10 keV is dominated by the jet or by the corona).

4 Simulations

In order to show the capabilities of SIMBOL-X, some simulations of well-known ULX spectra are presented here. The simulations were performed by using `xspec v 11.3.0` and the latest version of response matrices of SIMBOL-X (18 February 2004).

4.1 M81 X-9 or Holmberg IX X-1

This is one of the most famous ULX (Fig. 2): it was originally thought to belong to M81, but later on it was associated to the dwarf irregular galaxy Holmberg IX, distant from us 3.4 Mpc. According to Miller et al. (2003) it should be powered by a black hole of some hundreds of solar masses, depending on the model employed in the spectral fit.

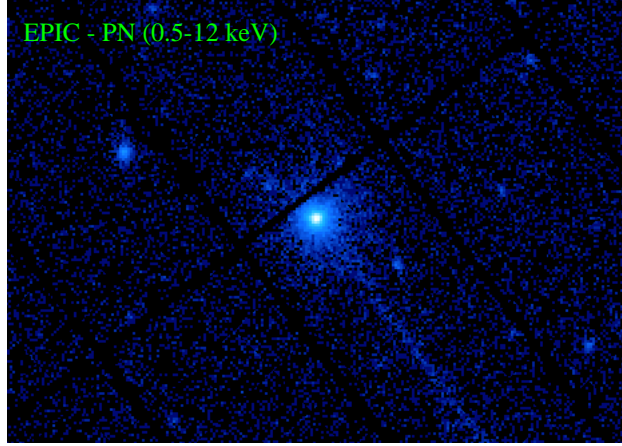


Figure 2: *XMM-Newton* EPIC-PN image of Holmberg IX X-1 in the energy band $0.5 - 12$ keV.

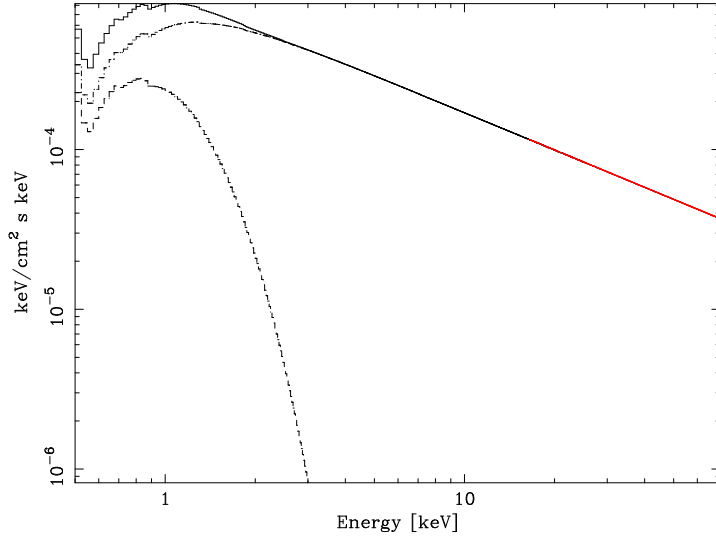


Figure 3: Model employed in the simulated spectrum of Holmberg IX X-1.

To perform the present simulations we started from the model suggested by Miller et al. (2003), that is the typical ULX model: a multicolor black body plus a power law (`wa(diskbb+po)` in `xspec`). The values are: $N_H = (2.3 \pm 0.3) \cdot 10^{21} \text{ cm}^{-2}$, $T_{in} = 0.26 \pm 0.05 \text{ keV}$, $\Gamma = 1.73 \pm 0.08$. The mass of the central object, inferred from the normalization of the multicolor black body, is $M \approx 330 M_\odot$. The flux, in the energy band $0.3 - 10 \text{ keV}$, is $8 \cdot 10^{-12} \text{ erg cm}^{-2} \text{ s}^{-1}$. More details and additional models can be found in Miller et al. (2003).

We simulated an observation of Holmberg IX X-1 with SIMBOL-X with an exposure of $2 \cdot 10^5 \text{ s}$. The obtained overall spectrum allows to refine the parameters: $N_H = (2.37^{+0.09}_{-0.08}) \cdot 10^{21} \text{ cm}^{-2}$, $T_{in} = 0.25 \pm 0.01 \text{ keV}$, $\Gamma = 1.778 \pm 0.009$. From the normalization of `diskbb`, we infer a mass of $M \approx 220 M_\odot$.

4.2 NGC1313 X-1

NGC1313 is a spiral galaxy (Hubble type SB(s)d) distant 3.7 Mpc, hosting two well known ULX (X-1 and X-2, Fig. 4). Miller et al. (2003) suggested that both could be powered by intermediate mass black holes.

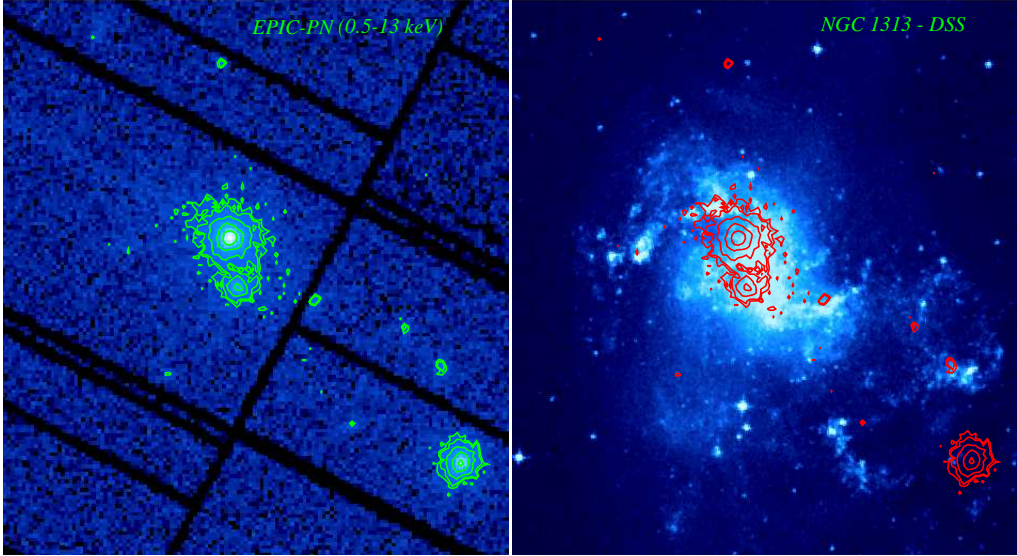


Figure 4: (left) *XMM-Newton* EPIC-PN image of NGC1313 X-1 in the energy band $0.5 - 13$ keV, with contours superimposed. (right) Optical image of NGC 1313 from the Digitized Sky Survey, with contours from the EPIC-PN image superimposed.

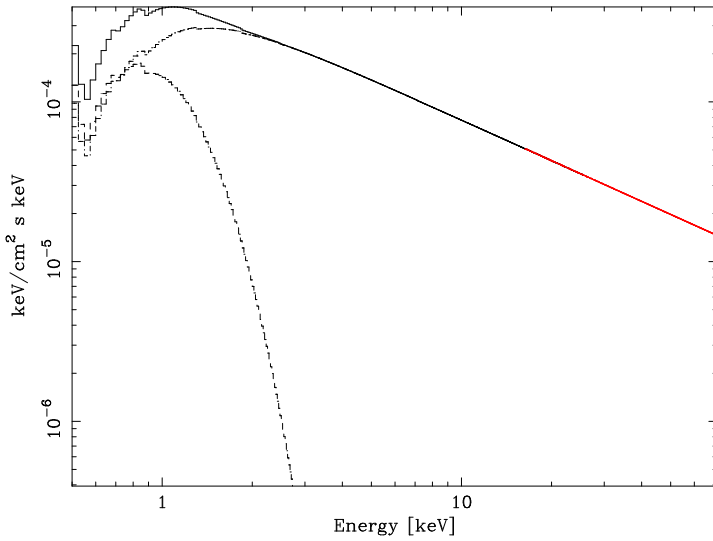


Figure 5: Model employed in the simulated spectrum of NGC1313 X-1.

For the present simulation we considered only NGC1313 X-1, starting from the model suggested by Miller et al. (2003): again, a multicolor black body plus a power law (`wa(diskbb+po)` in `xspec`). This time, the values are: $N_H = (3.1 \pm 0.3) \cdot 10^{21} \text{ cm}^{-2}$, $T_{in} = 0.23 \pm 0.03 \text{ keV}$, $\Gamma = 1.76 \pm 0.07$. The mass of the central object, inferred from the normalization of the multicolor black body, is $M \approx 400 M_\odot$. The flux, in the energy band $0.3 - 10$ keV, is $4.3 \cdot 10^{-12} \text{ erg cm}^{-2} \text{ s}^{-1}$. More details and additional models can be found in Miller et al. (2003).

Also in this case, we simulated an observation of NGC1313 X-1 with SIMBOL-X with an exposure of $2 \cdot 10^5$ s. The obtained overall spectrum allows to refine the parameters: $N_H = (3.3^{+0.2}_{-0.1}) \cdot 10^{21} \text{ cm}^{-2}$, $T_{in} = 0.21 \pm 0.01 \text{ keV}$, $\Gamma = 1.85 \pm 0.01$. From the normalization of `diskbb`, we infer a mass of $M \approx 360 M_\odot$.

4.3 M33 X-8

M33 is a well-known spiral galaxy (Hubble type SA(s)cd) distant from us only 795 kpc. The source X-8 is placed close to the dynamical centre (less than 2.3 pc, found with *Chandra* – Dubus & Rutledge 2002), but presently no telescope is able to resolve the nuclear region and the optical counterpart is still unknown.

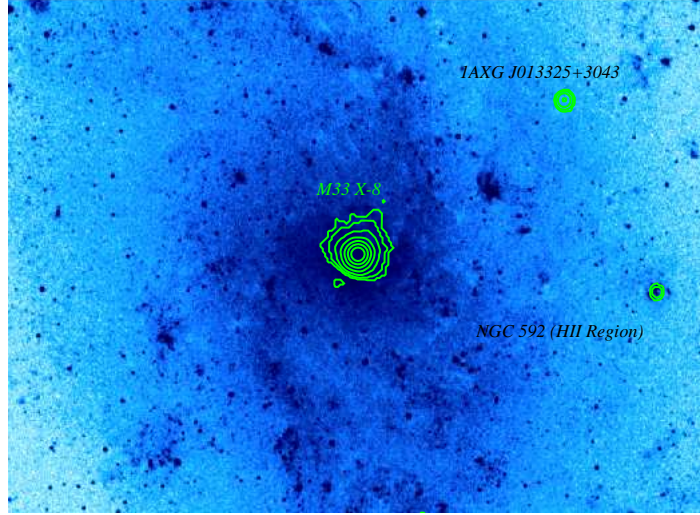


Figure 6: Optical image of M33 from the Digitized Sky Survey, with contours from the EPIC-PN superimposed (energy band 0.5 – 10 keV).

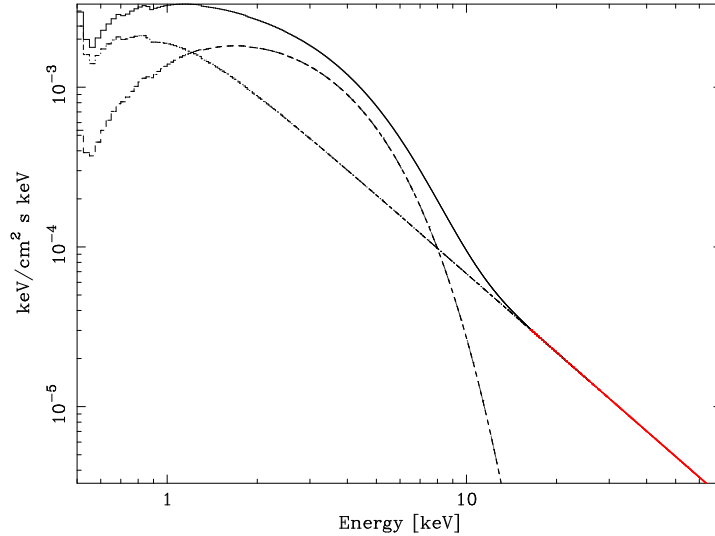


Figure 7: Model employed in the simulated spectrum of M33 X-8.

M33 X-8 is one of the typical ULX with the “too hot” disk. In this case, the values of the usual model (`wa(diskbb+po)` in `xspec`) are: $N_H = (1.8 \pm 0.2) \cdot 10^{21} \text{ cm}^{-2}$, $T_{in} = 1.16 \pm 0.04 \text{ keV}$, $\Gamma = 2.5 \pm 0.2$. The mass of the central object, inferred from the normalization of the multicolor black body, is $M \approx 12 M_\odot$. The flux, in the energy band 0.5 – 10 keV, is $1.7 \cdot 10^{-11} \text{ erg cm}^{-2} \text{ s}^{-1}$. More details and additional models can be found in Foschini et al. (2004).

Also in this case, the simulated observation (with an exposure of $2 \cdot 10^5 \text{ s}$), allows to refine the spectral parameters: $N_H = (1.91 \pm 0.04) \cdot 10^{21} \text{ cm}^{-2}$, $T_{in} = 1.184 \pm 0.007 \text{ keV}$, $\Gamma = 2.64 \pm 0.01$.

5 Final remarks

We presented here some simulations to show the capabilities of SIMBOL-X in the research field of ULX. The availability of a broad band spectrum (0.5 – 70 keV) allow to put better constraints in the spectral parameters. Moreover, this could be particularly useful in the case of presence of collimated emission and the interaction with the circumstellar environment (see e.g. Markoff et al. 2001). However, it is worth mentioning that the HEW and sensibility of SIMBOL-X at energies greater than 10 keV would allow to study for the first time the ULX in this energy range. Therefore, surprises are expected.

References

- [1] Begelman M.C., 2002, ApJ, 568, L100.
- [2] Dubus G., Rutledge R.E., 2002, MNRAS, 336, 901.
- [3] Dunne B.C. et al., 2000, ApJ, 119, 1172
- [4] Ebisawa K. et al., 2003, ApJ, 597, 780.
- [5] Fabbiano G., 1989, ARA&A, 27, 87.
- [6] Fabbiano G. et al., 2001, ApJ, 554, 1035.
- [7] Ferrando P. et al., 2003, SIMBOL-X: a new generation hard X-ray telescope, *Proceedings of SPIE* 5168, San Diego, August 2003.
- [8] Foschini L. et al., 2002a, A&A, 392, 817.
- [9] Foschini L. et al., 2002b, A&A, 396, 787.
- [10] Foschini L. et al., 2004, A&A, 416, 529.
- [11] Georganopoulos M. et al., 2002, A&A, 388, L25.
- [12] Hasinger G., 2004, Evolution of the sources of the X-ray Background, *First SIMBOL-X Workshop*, Paris, 11 – 12 March 2004.
- [13] Kaaret P. et al., 2003, Science 299, 365.
- [14] King A.R. et al., 2001, ApJ, 552, L109.
- [15] Kubota A. et al., 1998, PASJ, 50, 667.
- [16] Makishima K. et al., 2000, ApJ, 535, 632.
- [17] Markoff S. et al., 2001, A&A, 372, L25.
- [18] Miller J.M. et al., 2003a, ApJ, 585, L37.
- [19] Miller J.M. et al., 2003b, ApJ, accepted for publication ([astro-ph/0310617](#)).
- [20] Miller M.C., Colbert E.J.M., 2004, Int. J. Mod. Phys., D13, 1.
- [21] Schlegel E.M., 1994, ApJ, 424, L99.
- [22] Shimura T. & Takahara F., 1995, ApJ, 445, 780.
- [23] Wang D.Q. et al., 2004, ApJ, accepted for publication ([astro-ph/0403413](#)).